Eurographics Symposium on Geometry Processing 2014
Thomas Funkhouser and Shi-Min Hu
(Guest Editors)

Volume 33 (2014), Number 5

Semi-sharp Creases on Subdivision Curves and Surfaces

J. Kosinka[1], M. A. Sabin[2], and N. A. Dodgson[1]

[1]University of Cambridge, UK
[2]Numerical Geometry Ltd, Ely, UK

Abstract

We explore a method for generalising Pixar semi-sharp creases from the univariate cubic case to arbitrary degree subdivision curves. Our approach is based on solving simple matrix equations. The resulting schemes allow for greater flexibility over existing methods, via control vectors. We demonstrate our results on several high-degree univariate examples and explore analogous methods for subdivision surfaces.

Categories and Subject Descriptors (according to ACM CCS): Computer Graphics [I.3.5]: Computational Geometry and Object Modeling—Curve, surface, solid, and object representations

1. Introduction

Subdivision is a popular technique for modelling curves and surfaces, especially in the context of computer games and animated films. While other families of schemes exist, the most popular surface schemes are based on tensor-product B-splines (Catmull-Clark scheme [CC78]) or box-splines (Loop's scheme [Loo87]). Subdivision curves play an important role, too, as they are found on surfaces as boundary curves and creases, and bivariate subdivision rules are derived from the underlying univariate rules.

Subdivision curves and surfaces are essentially parametric objects and efficient evaluation algorithms exist [Sta98]. This then allows for shapes modelled using subdivision to be used not only in modelling, but also in finite element analysis [COS00]. As subdivision curves and surfaces are typically smooth everywhere, creases need to be modelled explicitly and require modified subdivision rules. In particular for the case of Catmull-Clark subdivision, this was elegantly addressed by Pixar in [DKT98], including support for semi-sharp creases, which appear naturally on real-world objects.

Subdivision schemes have been generalised to support arbitrary degrees [Sta01] in the uniform setting and also to non-uniform subdivision surfaces [Cas10] using multi-stage algorithms, motivated, in the latter case, by the desire to make NURBS and subdivision compatible. However, semi-sharp creases, an important modelling ingredient, are not, in general, available for higher degree subdivision shapes.

Building on the method developed in [KSD14b], we identify a family of univariate schemes that support modelling with semi-sharp creases and show that the resulting schemes generalise the odd-degree rules proposed in [Sta01] to arbitrary degrees (Sec. 3). Extending the traditional spline formulation by control vectors [KSD14a], we devise a framework for incorporating control vectors in arbitrary degree subdivision curves that is suited for modelling with semi-sharp creases (Sec. 4). Based on our univariate results, we initiate the study of supporting modelling with semi-sharp creases on arbitrary-degree subdivision surfaces facilitated by control vectors (Sec. 5). We demonstrate the capabilities of our method on several univariate and bivariate examples and we address the limitations and advantages of our approach (Sec. 6). We start by discussing related work.

2. Related work

Creases on curves and surfaces play an important role in modelling. Moreover, if we try to fit a smooth shape to an object with a crease, we will get unwanted undulations [HDD*94]. A comparison of approaches to modelling with creases is presented in [KSD14b]. While primarily focused on the curve case, most results generalise to surfaces. Tools for handling boundaries and creases on spline surfaces include knot insertion, ghost points, and multiple control points. However, modifying subdivision rules is a superior method, especially in the surface case, as it can be applied locally and no new control points need to be introduced [KSD14c]. The semi-sharp crease rules proposed by Pixar [DKT98] are a prime example.

Nevertheless, Pixar semi-sharp creases are limited to Catmull-Clark surfaces. A multi-stage approach was introduced by Stam [Sta01]. While Stam's approach works for any degree, sharp creases are limited to odd degrees and, as we show below, the method results into undesirable end-conditions. Cashman's "NURBS-compatible subdivision" [CADS09, Cas10] allows multiple knot lines, and thus creases, but they need to run across the whole surface (or form closed loops). Kosinka et al. extend Cashman's method to allow knot lines and creases to be truncated [KSD14c], but the approach is based on knot insertion and thus introduces unnecessary control points, especially on higher-degree surfaces.

Other constructions with crease support include NURSS [SZSS98], the schemes by Müller et al. [MRF06, MFR*10], and extended Doo-Sabin subdivision [HW11]. However, all these constructions are limited to degrees up to three.

A matrix-based approach to creases on arbitrary-degree subdivision curves was introduced in [KSD14b]. Building on that we show how to generalise Stam's odd-degree sharp creases to arbitrary-degree semi-sharp creases. Moreover, we combine this with control vectors introduced in [KSD14a] and produce new families of arbitrary-degree schemes with support for semi-sharp creases.

3. Creases on subdivision curves

To fix notation and to be able to build on top of previous work, we briefly recall the approach to creases taken in [KSD14b]. Our investigations apply to arbitrary degree subdivision. We also propose a new quintic scheme suitable for modelling curves with semi-sharp creases and reveal a link between the methods of [Sta01] and [KSD14b].

3.1. A matrix approach to creases

Denote $\mathbf{B} = (B_{0,d}(t), B_{1,d}(t), \ldots)$ the vector of uniform B-splines [dB72] of degree d defined over the knot vector

$$\mathbf{t} = [\underbrace{0, \ldots, 0}_{(d+1)\times}, 2, 4, 6, 8, \ldots].$$

Note that $t = 0$ corresponds to a boundary point; crease rules and basis functions can be obtained from boundary rules and functions by symmetry. In order to select a subspace of the space spanned by $\mathbf{B}$, a selection matrix $\mathbf{M}$ is used to construct $\mathbf{N} = \mathbf{BM} = (N_{0,d}, N_{1,d}, \ldots)$, a basis that can still represent a sharp crease, but with fewer basis functions than in $\mathbf{B}$ for $d \geq 3$. This simplifies the resulting subdivision rules and avoids unnecessary control points otherwise created using, for example, knot insertion.

Since $\mathbf{B}$ is refinable, a subdivision matrix $\mathbf{S}$ exists such that $\mathbf{B} = \mathbf{bS}$, where $\mathbf{b}$ is the refined basis over the finer knot vector

$$\boldsymbol{\tau} = [\underbrace{0, \ldots, 0}_{(d+1)\times}, 1, 2, 3, 4, \ldots].$$

In addition, $\mathbf{N}$ has to be refinable as well, so $\mathbf{N} = \mathbf{nT}$ for some subdivision matrix $\mathbf{T}$, where $\mathbf{n}$ is the refined version of $\mathbf{N}$. Moreover, it holds $\mathbf{n} = \mathbf{bM}$ over $\boldsymbol{\tau}$.

From the four matrix equations

$$\mathbf{N} = \mathbf{BM}, \quad \mathbf{B} = \mathbf{bS}, \quad \mathbf{N} = \mathbf{nT}, \quad \mathbf{n} = \mathbf{bM} \tag{1}$$

and the fact that $\mathbf{b}$ forms a basis it follows that

$$\mathbf{SM} = \mathbf{MT}. \tag{2}$$

For a fixed degree d, $\mathbf{S}$ is known; it is the subdivision matrix for B-splines at a knot of multiplicity $d+1$. Thus, (2) needs to be solved for $\mathbf{M}$ and $\mathbf{T}$; this yields a system of bilinear equations. This approach can be applied to higher degree schemes, including even degrees; see [KSD14b] for details.

For example in the case of cubics, the Pixar (infinitely sharp) crease rule is one solution of (2) with

$$\mathbf{M}_3 = \begin{pmatrix} 1 & 0 & 0 & \\ \frac{2}{3} & \frac{1}{3} & 0 & \\ 0 & 1 & 0 & \\ 0 & 0 & 1 & \\ & & & \ddots \end{pmatrix}, \mathbf{T}_3 = \frac{1}{8}\begin{pmatrix} 8 & 0 & 0 & 0 & \\ \mathbf{4} & \mathbf{4} & 0 & 0 & \\ \mathbf{1} & \mathbf{6} & \mathbf{1} & 0 & \\ 0 & \mathbf{4} & \mathbf{4} & 0 & \\ & & & & \ddots \end{pmatrix}. \tag{3}$$

The rows in bold in $\mathbf{T}_3$ correspond to regular subdivision stencils not influenced by the crease. Only the first stencil (row) of $\mathbf{T}_3$ is different; all the other stencils are regular. This gives the smooth rule $[1,6,1]/8$ and the sharp rule $[8]/8 = [1]$ for new vertex points as described in [DKT98]. New edge points are always computed using $[4,4]/8$. For the semi-sharp generalisation, each original vertex is associated with a sharpness value, s, which indicates how many times the sharp rule is used for that vertex before switching to the smooth rule as subdivision proceeds. This results in semi-sharp creases. Non-integer values of s can also be supported by linear interpolation. This is the univariate version of Pixar semi-sharp creases [DKT98].

We note that this approach (Eq. (2)) resembles the lofting method of Schaefer et al. [SWZ04] (see their Eq. (1)). However, we focus on creating new subdivision rules at boundaries and creases, while they consider lofting and interpolation. The difference is most evident in matrix $\mathbf{M}$: in [SWZ04] it is a *known* change-of-basis matrix but here it is an *unknown* subspace-selection matrix.

3.2. Semi-sharp rules for higher degrees

In order to generalise this to higher degrees, we need to be able to switch between the sharp rule and the smooth rule.

However, because stencils get larger with degree and more of them become irregular near creases, a different approach needs to be taken. We explore two options. First, one can use the multi-stage approach of Stam [Sta01]. Second, one can adapt the approach taken in [KSD14b] by breaking some of the rules imposed therein. As we show below, both options give the same answer in the case of odd degrees.

3.2.1. Quintics

The matrix equation (2) leads in the quintic case to three different subdivision matrices; see Section 4.2 in [KSD14b]. However, the first three stencils are not regular in any of the three cases. This fact complicates implementation, but more importantly it prevents the direct use of the (semi-)sharp approach from the cubic case, because the sharp rule influences points other than the sharp control point itself; in particular two adjacent sharp control points require special treatment.

We therefore investigate ways to modify stencils to obtain only few irregular ones in $\mathbf{T}$ by breaking some of the conditions imposed on $\mathbf{M}$ and/or $\mathbf{T}$ in Section 3 of [KSD14b]. In particular, we can relax only conditions (M3) and (T3) from [KSD14b] to obtain larger solution spaces without compromising the integrity of the approach.

For $d=5$, we relax $\mathbf{M}$ and $\mathbf{T}$ (omitting $\ddots$) to

$$\mathbf{M}_5 = \begin{pmatrix} 1 & 0 & 0 \\ m_1 & m_2 & \mathbf{1-m_1-m_2} \\ m_3 & m_4 & 1-m_3-m_4 \\ 0 & m_5 & 1-m_5 \\ 0 & 0 & 1 \end{pmatrix}, \qquad \mathbf{T}_5 = \tfrac{1}{32}\begin{pmatrix} 32 & 0 & 0 & 0 \\ t_1 & t_2 & \mathbf{32-t_1-t_2} & 0 \\ \mathbf{6} & \mathbf{20} & \mathbf{6} & 0 \\ \mathbf{1} & \mathbf{15} & \mathbf{15} & \mathbf{1} \end{pmatrix}, \tag{4}$$

where the elements in bold red violate conditions (M3) and (T3) from [KSD14b], respectively. This then leads, via (2), to a linear system with the unique solution

$$\mathbf{M}_5 = \begin{pmatrix} 1 & 0 & 0 \\ \frac{49}{60} & \frac{1}{6} & \mathbf{\frac{1}{60}} \\ \frac{9}{20} & \frac{1}{2} & \frac{1}{20} \\ 0 & \frac{4}{5} & \frac{1}{5} \\ 0 & 0 & 1 \end{pmatrix}, \mathbf{T}_5 = \frac{1}{32}\begin{pmatrix} 32 & 0 & 0 & 0 \\ 17 & 14 & \mathbf{1} & 0 \\ \mathbf{6} & \mathbf{20} & \mathbf{6} & 0 \\ \mathbf{1} & \mathbf{15} & \mathbf{15} & \mathbf{1} \end{pmatrix}. \tag{5}$$

Note that already the third stencil in $\mathbf{T}_5$ is regular. The spectrum of $\mathbf{T}_5$ is $(1, \frac{1}{2}, \frac{1}{8}, \frac{1}{32}, 0, 0, \ldots)$ and the subdominant unnormalised right eigenvector reads $\mathbf{v}_1 = (0,1,2,3,4,5,6,7)$. In other words, the natural configuration at $t=0$ is linear, giving a good distribution of points near creases and endpoints as subdivision proceeds. The end-conditions for the corresponding spline curve $\mathbf{c}(t) = \sum_{i=0}^{n-1} N_{i,5}(t)\mathbf{P}_i$ are

$$\begin{aligned} \mathbf{c}(0) &= \mathbf{P}_0, \\ \mathbf{c}'(0) &= \tfrac{1}{12}(-11\mathbf{P}_0 + 10\mathbf{P}_1 + \mathbf{P}_2), \\ \mathbf{c}''(0) &= \mathbf{0}. \end{aligned} \tag{6}$$

Note that $\mathbf{P}_2$ influences the first derivative at $t=0$ and thus the tangent there. This behaviour is typically regarded as problematic. However, since the weight of $\mathbf{P}_2$ in $\mathbf{c}'(0)$ is relatively small, the tangent of $\mathbf{c}$ at $t=0$ does not deviate far from $\overline{\mathbf{P}_0\mathbf{P}_1}$. This issue is partially redeemed by the fact that the stencils (rows) in $\mathbf{T}_5$ go back to the uniform quintic stencils $[6,20,6]/32$ and $[1,15,15,1]/32$ almost immediately, in contrast to the quintic solutions given in Section 4.2 of [KSD14b] where the first six stencils are all irregular. Consequently, the scheme given by $\mathbf{T}_5$ is easy to implement using stencils. Adjacent crease points, however, need special care: the new control point introduced between two crease points in the first subdivision step has to use the stencil $[16,16]/32$ to ensure symmetry (Fig. 1). An example with semi-sharp creases on a quintic spline is shown in Fig. 2.

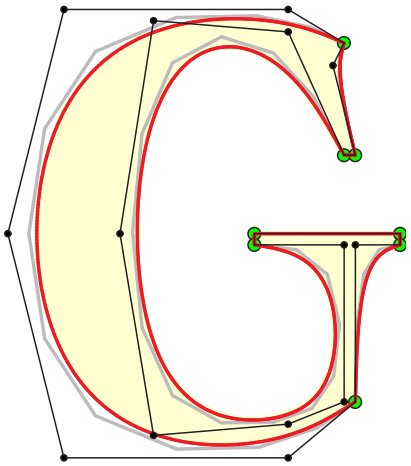

Figure 1: *The letter G designed using our quintic scheme governed by $\mathbf{T}_5$. Note that the scheme properly handles any configuration of control points marked as sharp (green). The control polygon after one subdivision step is shown in grey.*

To fix the issue with the end-conditions in (6), one can show different control points to the user from those that are used internally. In the particular case of $\mathbf{T}_5$, one can keep $\mathbf{P}_1$ internally, but replace it with $\tilde{\mathbf{P}}_1 = (10\mathbf{P}_1 + \mathbf{P}_2)/11$ for the user (Fig. 3). The inverse transform is then simply $\mathbf{P}_1 = (11\tilde{\mathbf{P}}_1 - \mathbf{P}_2)/10$. An alternative would be to project $\mathbf{P}_1$ onto the line given by $\mathbf{P}_0, \tilde{\mathbf{P}}_1$ and use the foot point instead of $\tilde{\mathbf{P}}_1$, thus minimising the adjustment of $\mathbf{P}_1$ required.

Interestingly, one can express this quintic solution using ghost points [LB07, KSD14b]. It can be verified that setting $\mathbf{P}_{-1} = 2\mathbf{P}_0 - \mathbf{P}_1$ and $\mathbf{P}_{-2} = 2\mathbf{P}_0 - \mathbf{P}_2$ gives the same quintic

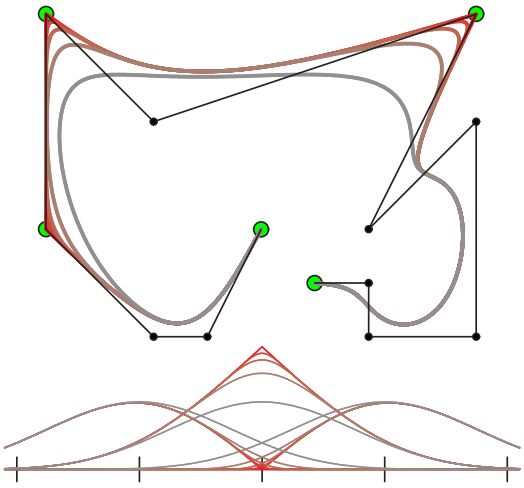

Figure 2: *A degree 5 subdivision curve given by $\mathbf{T}_5$ in (5) with semi-sharp creases with $s \in \{0,1,2,3,\infty\}$ (grey to red) for the three internal vertices marked as sharp (green). Boundary vertices are handled as infinitely sharp. Note that the scheme deals with consecutive sharp control points. Five sets of three basis functions at a crease are shown at the bottom, ranging from smooth ($s=0$; in grey) to (infinitely) sharp ($s=\infty$; in red).*

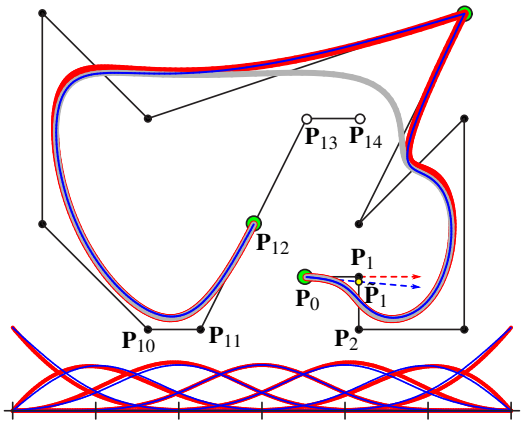

Figure 3: *A comparison of end-conditions in the quintic case. The red curve and basis functions are given by (29) in [KSD14b]; cf. Fig. 5 therein. The corresponding smooth curve with no internal points marked as sharp is shown in grey as reference. The curve and basis functions given by $\mathbf{T}_5$ in (5) are shown in blue. Note the difference between the red and blue tangents (dashed lines) at $\mathbf{P}_0$. The tangent of the blue curve can be forced to be given by the first two control points by displaying $\tilde{\mathbf{P}}_1$ instead of the original control point $\mathbf{P}_1$ to the user. The points $\mathbf{P}_{13}$ and $\mathbf{P}_{14}$ are ghost points.*

basis (Fig. 3). Further, one can verify that $\mathbf{T}_5$ results from $\mathbf{T}_3$ by applying the smoothing rule $[1,2,1]/4$ (the first element is kept fixed) of [Sta01] to it. Therefore, Stam's scheme and our quintic scheme (5) with creases are equivalent.

3.2.2. A modified quintic scheme

We explore one more idea. Turning back to (5) and the fact that handling neighbouring creases requires the stencil $[16,16]/32$ brings us to the modified matrix

$$\bar{\mathbf{T}}_5 = \frac{1}{32}\begin{pmatrix} 32 & 0 & 0 & 0 \\ \mathbf{16} & \mathbf{16} & 0 & 0 \\ \mathbf{6} & \mathbf{20} & \mathbf{6} & 0 \\ \mathbf{1} & \mathbf{15} & \mathbf{15} & \mathbf{1} \\ 0 & \mathbf{6} & \mathbf{20} & \mathbf{6} \end{pmatrix}. \tag{7}$$

This quintic scheme handles any configuration of creases easily and the (one directional) tangent at a boundary point (crease) is given by only two control points, as typically required in modelling. On the other hand, since $\bar{\mathbf{T}}_5$ is not a solution of (2), the resulting curve consists of infinitely many quintic pieces joined with C^4 continuity in the neighbourhoods of boundaries and creases. An example is shown in Fig. 4. This scheme is easy to implement, including support for semi-sharp creases, and thus more suitable for applications in modelling and graphics than the scheme given in (5).

The behaviour of this modified scheme resembles that of subdivision surfaces near extraordinary points and can be considered inferior to the scheme given in (5). However, Stam's approach [Sta98] to evaluating subdivision surfaces still applies and thus the subdivision scheme given by $\bar{\mathbf{T}}_5$ can be used in finite element analysis as well.

3.2.3. Degrees 7 and higher

Proceeding similarly for $d=7$, one arrives at

$$\mathbf{M}_7 = \begin{pmatrix} 1 & 0 & 0 & 0 \\ \frac{1109}{1260} & \frac{7}{72} & \mathbf{\frac{1}{45}} & \mathbf{\frac{1}{2520}} \\ \frac{269}{420} & \frac{7}{24} & \frac{1}{15} & \mathbf{\frac{1}{840}} \\ \frac{32}{105} & \frac{113}{210} & \frac{16}{105} & \frac{1}{210} \\ 0 & \frac{25}{42} & \frac{8}{21} & \frac{1}{42} \\ 0 & 0 & \frac{6}{7} & \frac{1}{7} \\ 0 & 0 & 0 & 1 \end{pmatrix} \tag{8}$$

and

$$\mathbf{T}_7 = \frac{1}{128}\begin{pmatrix} 128 & 0 & 0 & 0 & 0 \\ 72 & 48 & \mathbf{8} & 0 & 0 \\ 30 & 69 & 28 & \mathbf{1} & 0 \\ \mathbf{8} & \mathbf{56} & \mathbf{56} & \mathbf{8} & 0 \\ \mathbf{1} & \mathbf{28} & \mathbf{70} & \mathbf{28} & \mathbf{1} \end{pmatrix}. \tag{9}$$

The fourth stencil of $\mathbf{T}_7$ is regular, in contrast to the tenth stencil in the solution presented in [KSD14b] being the first regular one. The spectrum of $\mathbf{T}_7$ is $(1, \frac{1}{2}, \frac{1}{8}, \frac{1}{32}, \frac{1}{128}, 0, 0, \ldots)$

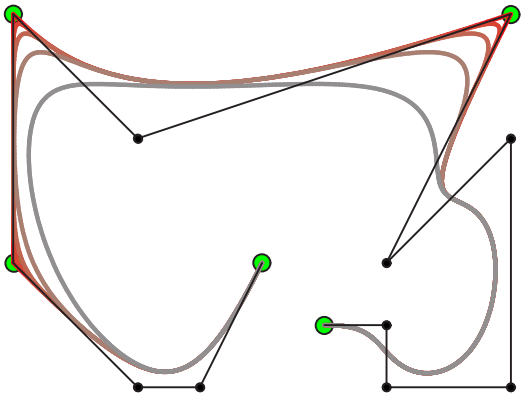

Figure 4: *A modified quintic spline with semi-sharp creases governed by* $\tilde{\mathbf{T}}_5$*; cf. Fig. 2.*

and the natural configuration at $t = 0$ is linear. The end-conditions are

$$\begin{aligned} \mathbf{c}(0) &= \mathbf{P}_0, \\ \mathbf{c}'(0) &= \tfrac{1}{360}(-302\mathbf{P}_0 + 245\mathbf{P}_1 + 56\mathbf{P}_2 + \mathbf{P}_3), \\ \mathbf{c}''(0) &= \mathbf{0}. \end{aligned} \tag{10}$$

Note that four control points influence the tangent at $t = 0$. By displaying $\tilde{\mathbf{P}}_1 = (245\mathbf{P}_1 + 56\mathbf{P}_2 + \mathbf{P}_3)/302$ instead of $\mathbf{P}_1$, the effect of the extra two control points on the tangent at $t = 0$ can (as in the quintic case) be hidden from the user.

As with the degree five scheme above, one can use ghost points again. Their positions are given by $\mathbf{P}_{-i} = 2\mathbf{P}_0 - \mathbf{P}i$, $i = 1,2,3$. And again, $\mathbf{T}_7$ can be obtained from $\mathbf{T}_5$ by the smoothing rule $[1,2,1]/4$. We have checked that both these properties generalise for odd degrees up to 17 with $i = 1,2,\ldots,(d-1)/2$. It is therefore reasonable to expect that they hold for arbitrary odd degrees. While Stam's method for creases is limited to odd degrees, the matrix approach works for arbitrary degrees. For example, when $d = 4$, we obtain

$$\mathbf{M}_4 = \begin{pmatrix} 1 & 0 & 0 & 0 \\ \frac{2}{3} & \frac{1}{4} & \frac{1}{12} & 0 \\ 0 & \frac{3}{4} & \frac{1}{4} & 0 \\ 0 & 0 & 1 & 0 \end{pmatrix}, \mathbf{T}_4 = \frac{1}{16}\begin{pmatrix} 16 & 0 & 0 & 0 \\ 10 & 5 & 1 & 0 \\ 2 & 9 & 5 & 0 \\ 0 & 5 & 10 & 1 \end{pmatrix}.$$

We remark that the matrix approach can be used to determine whether a scheme described by $\mathbf{T}$ leads to piece-wise polynomial curves over the knot vector of $\mathbf{B}$. Since $\mathbf{S}$ is known, then for a given $\mathbf{T}$ the system $\mathbf{SM} = \mathbf{MT}$ yields a system of linear equations. If there exists a solution to this system, $\mathbf{T}$ produces piece-wise polynomial limit curves; see also Section 20 of [Sab10]. One example, with a positive answer, is the above mentioned family of odd degree schemes with creases developed by Stam [Sta01]. This polynomial nature of Stam's creases was previously unknown.

We now turn our attention to the use of control vectors to model semi-sharp creases on arbitrary-degree subdivision curves, as that avoids some of the problems encountered above and offers greater modelling flexibility.

4. Control vectors for subdivision curves

In [KSD14a], the traditional concept of splines based on control points is extended to include control vectors as well. More precisely, in the univariate case the general form is

$$\mathbf{c}(t) = \sum_{i=1}^{n} B_i(t)P_i + \sum_{j=1}^{m} C_j(t)V_j, \tag{11}$$

where P_i are control points, but V_j are understood as control vectors. In the same paper, it is also shown that this construction can be used to generalise Pixar semi-sharp rules by using uniform cubic B-splines for $B_i(t)$ and specific combinations of cubic B-splines for C_j governed by control vectors. As demonstrated in [KSD14a], control vectors present a new paradigm which offers greater modelling flexibility and is particularly well suited for modelling with semi-sharp creases. True multiresolution editing is supported because control vectors can be expressed in local adapted frames [FB88, KSD14a]. We emphasise that this goes beyond what Pixar and Stam's schemes offer.

We now generalise the cubic construction of [KSD14a] to support any degree subdivision with semi-sharp creases associated with control vectors. The approach is again based on matrices, but the ingredients are slightly different.

The basis $\mathbf{B}$ is now formed using B-splines of degree d

$$\mathbf{B} = \left(\ldots, B_{-2,d}(t), B_{-1,d}(t), B_{0,d}(t), B_{1,d}(t), B_{2,d}(t), \ldots\right)$$

centred around $t = 0$, the crease, over the knot vector

$$\mathbf{t} = (\ldots, -4, -2, \underbrace{0, \ldots, 0}_{d\times}, 2, 4, \ldots).$$

The refined basis defined over $\boldsymbol{\tau} = \mathbf{t}/2$ is denoted $\mathbf{b}$ with $\mathbf{B} = \mathbf{bS}$ as before. The new basis $\mathbf{N}$ we seek is composed of uniform B-splines $N_{i,d}$ defined over the knot vector $\mathbf{u} = (\ldots, -4, -2, 0, 2, 4, \ldots)$ plus an extra 'crease' basis function $\hat{N}_d$, i.e.,

$$\mathbf{N} = (\ldots, N_{-2,d}, N_{-1,d}, N_{0,d}, \hat{N}_d, N_{1,d}, N_{2,d}, \ldots).$$

The uniform B-splines are associated with control points and are thus able to represent any uniform spline, while the crease function is associated with a control vector. Since $\mathbf{N}$ spans a subspace of that spanned by $\mathbf{B}$, we have $\mathbf{N} = \mathbf{BM}$ and $\mathbf{n} = \mathbf{bM}$. To ensure refinability of $\mathbf{N}$, a subdivision matrix $\mathbf{T}$ must exist such that $\mathbf{N} = \mathbf{nT}$. Putting it all together, we again obtain that (2) has to hold. Due to the fact that the support width of a degree d uniform B-spline is $d+1$, we only need to consider finite matrices of the following sizes (rows × columns): $\mathbf{S}_{(2d+1)\times(2d+1)}$, $\mathbf{T}_{(d+3)\times(d+3)}$, and

$\mathbf{M}_{(2d+1)\times(d+3)}$. The remaining portions of the matrices consist of uniform subdivision rules in the cases of $\mathbf{S}$ and $\mathbf{T}$, and of unit matrices in the case of $\mathbf{M}$.

Let us take a closer look at the structure of the matrices involved. The subdivision matrix $\mathbf{S}$ is known and can be obtained using e.g. the Oslo algorithm [CLR80]. In the cubic case, the important portion of the matrix for our purposes is

$$\mathbf{S}_3 = \frac{1}{8}\begin{pmatrix} 1 & \frac{11}{2} & \frac{3}{2} & 0 & 0 & 0 & 0 \\ 0 & 2 & 6 & 0 & 0 & 0 & 0 \\ 0 & 0 & 4 & 4 & 0 & 0 & 0 \\ 0 & 0 & 0 & 8 & 0 & 0 & 0 \\ 0 & 0 & 0 & 4 & 4 & 0 & 0 \\ 0 & 0 & 0 & 0 & 6 & 2 & 0 \\ 0 & 0 & 0 & 0 & \frac{3}{2} & \frac{11}{2} & 1 \end{pmatrix}. \qquad (12)$$

The matrix $\mathbf{T}$ is the subdivision matrix for uniform B-splines of degree d augmented by an extra row and column to accommodate $\hat{N}_d$. The extra column contains unknown parameters t_i, $i = 1,\ldots,d+3$, which form the subdivision mask for $\hat{N}_d$. The extra row contains only zeros since $\hat{N}_d$ is the only crease function, except for the element shared with the extra column. In the cubic case,

$$\mathbf{T}_3 = \frac{1}{8}\left(\begin{array}{ccc|c|cc} 1 & 6 & 1 & t_1 & 0 & 0 \\ 0 & 4 & 4 & t_2 & 0 & 0 \\ 0 & 1 & 6 & t_3 & 1 & 0 \\ \hline 0 & 0 & 0 & t_4 & 0 & 0 \\ \hline 0 & 0 & 4 & t_2 & 4 & 0 \\ 0 & 0 & 1 & t_1 & 6 & 1 \end{array}\right) \qquad (13)$$

with the extra row and column delimited by lines. Note that due to symmetry, the number of parameters is reduced from 6 to 4, and from $d+3$ to $\lfloor d/2 \rfloor + 3$ for general degree d.

Finally, we treat $\mathbf{M}$. It is the subspace selection matrix from the B-spline basis defined over $\mathbf{t}$ to the uniform basis over $\mathbf{u}$ augmented by $\hat{N}_d$. It can thus be obtained by using knot insertion, up to the extra column corresponding to $\hat{N}_d$. The extra column contains unknown parameters m_j. Due to symmetry, support widths of B-splines, and the fact that the central element of the extra column is equal to 1 as $B_{0,d}$ is the only non-zero function in $\mathbf{B}$ at $t = 0$, the number of unknowns is equal to $\lfloor d/2 \rfloor$. In the cubic case,

$$\mathbf{M}_3 = \left(\begin{array}{ccc|c|cc} 1 & 0 & 0 & 0 & 0 & 0 \\ 0 & 1 & 0 & 0 & 0 & 0 \\ 0 & \frac{1}{3} & \frac{2}{3} & m_1 & 0 & 0 \\ 0 & \frac{1}{6} & \frac{2}{3} & 1 & \frac{1}{6} & 0 \\ 0 & 0 & \frac{2}{3} & m_1 & \frac{1}{3} & 0 \\ 0 & 0 & 0 & 0 & 1 & 0 \\ 0 & 0 & 0 & 0 & 0 & 1 \end{array}\right) \qquad (14)$$

with the extra column corresponding to $\hat{N}_d$ delimited by lines.

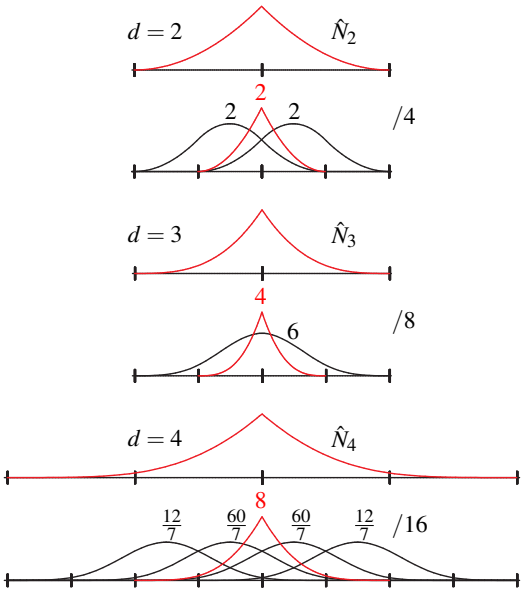

Figure 5: *Refinable crease functions $\hat{N}_d$ (red). For each degree, top rows show the original crease function and bottom rows show their refined version along with the uniform B-splines in $\mathbf{N}$ that contribute to the subdivision mask of $\hat{N}_d$.*

As in [KSD14b], the matrix equation $\mathbf{SM} = \mathbf{MT}$ yields a system of bilinear equations in terms of the unknowns t_i and m_j. While this system would give valid solutions, we impose further conditions to simplify it. First, we seek a crease function of minimal support. This reduces the number of m_j to $\lfloor d/2 \rfloor - 1$. Second, since $\hat{N}_d$ has to contain a sharp crease (i.e., $\hat{N}_d$ has to be C^0 at $t = 0$), we discard solutions for which $m_j = 1$ for any $j = 1,\ldots,\lfloor d/2 \rfloor - 1$. We consider only solutions satisfying both these conditions.

For $d = 3$ we obtain only one solution: $m_1 = t_1 = t_2 = 0$, $t_3 = 6$, $t_4 = 4$. As expected, the resulting N_4^0 is the cubic B-spline defined over $(-1,0,0,0,1)$; cf. Fig. 7 in [KSD14a].

For general d, the system $\mathbf{SM} = \mathbf{MT}$ leads (via a Gröbner basis computation) to a single polynomial equation of degree $\lfloor d/2 \rfloor$, all other equations are linear. The number of (real) solutions is $\lfloor d/2 \rfloor$, but only one satisfies all our requirements. The support width of the resulting $\hat{N}_d$ is $2\lfloor d/2 \rfloor$ and crease functions of smaller supports refinable with respect to $\mathbf{B} \cup \mathbf{N}$ do not exist. We tested that these results hold up to degree 17, and we conjecture that they generalise to arbitrary degree d.

A Maple script that includes the implementation of the algorithm, which takes an arbitrary degree as input and outputs the unique solution, is provided in the supplementary material. The matrices $\mathbf{M}$ and $\mathbf{T}$ for degrees up to 7 are also included.

The crease functions $\hat{N}_d$ and their subdivision masks, i.e.,

the extra column of $\mathbf{T}$, for degrees 2 to 4 are shown in Fig. 5. A degree 5 example is shown in Fig. 6. For the user interface, we find it natural to anchor start points of control vectors with limit points (red dots). The end points of control vectors are set to the corresponding control points in the case of odd degree schemes. In the cubic case, this directly generalises Pixar semi-sharp creases, as shown in [KSD14a]. As observed in [Sta01], creases in even degree schemes are not so natural. Therefore, we initialise control vector magnitudes to zero when d is even. A degree 4 example is shown in Fig. 7.

In contrast to other methods, including ghost points, knot insertion, and the crease rules developed in [KSD14b], our approach uses only two basis functions (up to translation) for any degree $d \geq 2$: the uniform B-spline and the crease function $\hat{N}_d$. Thus, only two masks are required to implement the scheme using control vectors: the uniform B-spline mask and the mask for $\hat{N}_d$, i.e., the extra column in $\mathbf{T}$. These are summarised in Table 1 for degrees up to 7.

Furthermore, our approach holds the following properties:

- Linear independence of basis functions. This follows from the fact that the only functions used are shifts of the uniform B-spline and the crease function $\hat{N}_d$.
- Any $d \geq 2$ is supported, including even degrees.
- Full polynomial reproduction and approximation power. This is provided by the underlying uniform B-spline basis. This is not the case for the Pixar method [DKT98] and Stam's approach [Sta01].

These features imply that our approach is more general and more flexible than the methods of [DKT98, Sta01].

As we aim to extend the cubic scheme to the surface case in the next section, we show the cubic stencils in Fig. 8.

5. Control vectors for subdivision surfaces

Our results from Section 4 generalise straightforwardly to tensor product surfaces. The underlying surface is a standard tensor-product B-spline surface and control vectors are then associated with tensor products of $B_i(t)$ and $C_j(t)$ from (11). Consequently, (11) becomes

$$\begin{aligned}\mathbf{s}(u,v) \quad = \quad & \textstyle\sum_{i=1}^{n}\sum_{j=1}^{m} B_i(u)B_j(v)P_{i,j} + B_i(u)C_j(v)U_{i,j} + \\ & C_i(u)B_j(v)V_{i,j} + C_i(u)C_j(v)X_{i,j},\end{aligned} \tag{15}$$

where $P_{i,j}$ form a rectangular array of control points. Vectors $U_{i,j}$ control local creases in the u-direction, $V_{i,j}$ in the v-direction, and $X_{i,j}$ control crossing creases. The associated types of basis functions in the bicubic case are shown in Fig. 9. However, we emphasise that this construction works for surfaces of general bi-degree $d_1 \times d_2$. Moreover, each control vector is associated with a sharpness value, initialised to zero; see Fig. 10.

In order to support arbitrary manifold topology and semi-sharp creases, we now turn our attention to extending the

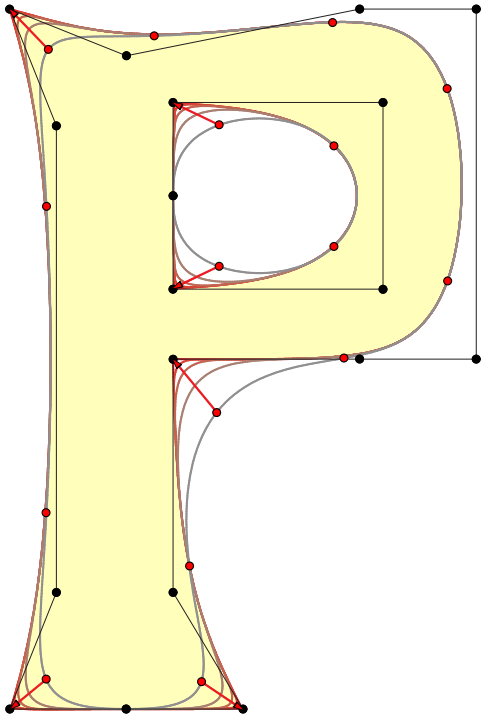

Figure 6: *The letter P created using our quintic scheme with semi-sharp creases controlled by vectors. The default setting of control vectors as differences between corresponding control points and limit points has been used in this example, but the user is free to modify that and to use various levels of sharpness independently.*

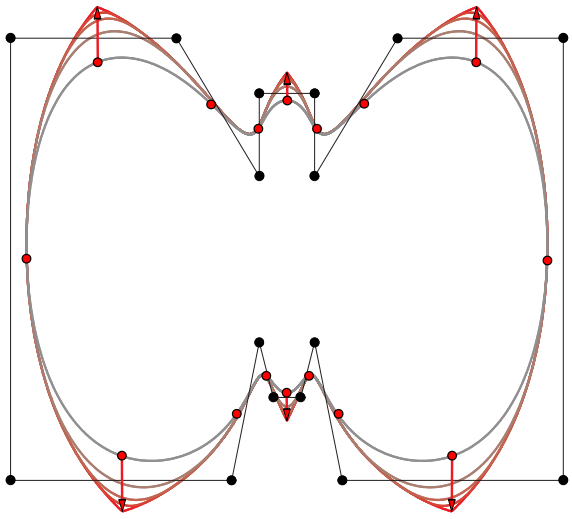

Figure 7: *A degree four spline with semi-sharp creases via control vectors. The red points are limit points. Creases are created when the control vector has non-zero length and its sharpness is non-zero.*

Table 1: *A table of masks for uniform B-splines B_d and the crease functions $\hat{N}_d$ for $d = 2,\ldots,7$. Since the contribution of $\hat{N}_d$ to its refined copy is always equal to $1/2$ (see Fig. 5, red), it is not included for clarity. Thus, all the listed mask contributions are to the scaled and translated copies of B_d.*

$d=2$	B_2	$[1,3,3,1]/4$
	$\hat{N}_2$	$[2,2]/4$
$d=3$	B_3	$[1,4,6,4,1]/8$
	$\hat{N}_3$	$[6]/8$
$d=4$	B_4	$[1,5,10,10,5,1]/16$
	$\hat{N}_4$	$[\frac{12}{7},\frac{60}{7},\frac{60}{7},\frac{12}{7}]/16$
$d=5$	B_5	$[1,6,15,20,15,6,1]/32$
	$\hat{N}_5$	$[\frac{30}{7},\frac{180}{7},\frac{30}{7}]/32$
$d=6$	B_6	$[1,7,21,35,35,21,7,1]/64$
	$\hat{N}_6$	$[\frac{360}{239},\frac{2520}{239},\frac{8640}{239},\frac{8640}{239},\frac{2520}{239},\frac{360}{239}]/64$
$d=7$	B_7	$[1,8,28,56,70,56,28,8,1]/128$
	$\hat{N}_7$	$[\frac{840}{239},\frac{6720}{239},\frac{25200}{239},\frac{6720}{239},\frac{840}{239}]/128$

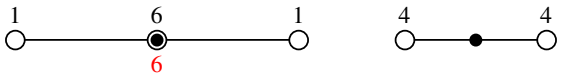

Figure 8: *Unnormalised cubic stencils for subdivision with control vectors. White points represent old vertices, black points mark new points after a refinement step. The top numbers (black) are contributions of control points, the lower 6 in red is the contribution from the corresponding control vector. All weights need to be normalised by $1/8$. The contribution of a control vector to its new vector is $1/2$ (not shown). Left: New vertex-point rule. Right: New edge-point rule.*

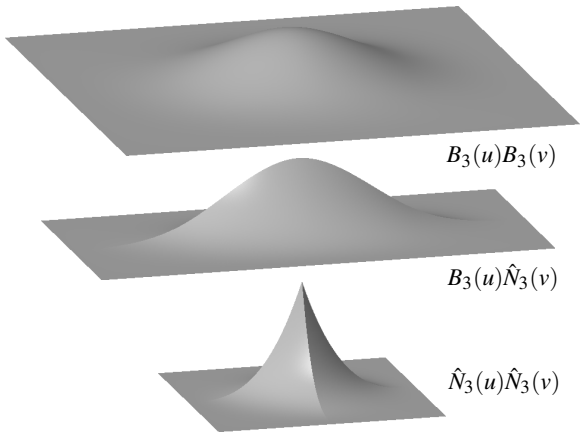

Figure 9: *Three shapes of bicubic basis functions. The fourth one, $\hat{N}_3(u)B_3(v)$, is a rotated version of $B_3(u)\hat{N}_3(v)$.*

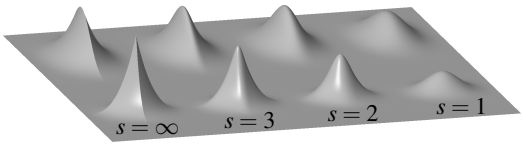

Figure 10: *Crease basis functions of various sharpness values s. Front row: $\hat{N}_3(u)\hat{N}_3(v)$. Back row: $\hat{N}_3(u)B_3(v)$.*

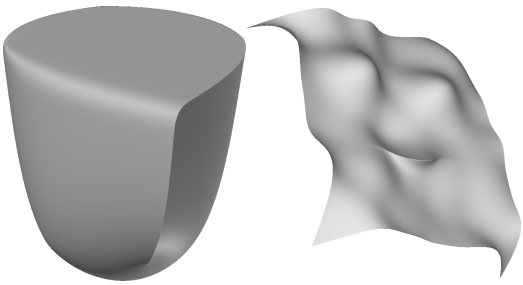

Figure 11: *Two examples of degree 5 subdivision surfaces with creases. Left: Sharp and semi-sharp creases on a cuboid model. Right: A vanishing crease created by a control vector associated with $N_5(u)\hat{N}_5(v)$.*

tensor product setting to subdivision surfaces. While higher (and especially odd) degrees could be considered (simple biquintic examples are shown in Fig. 11), we focus on the case of Catmull-Clark subdivision surfaces [CC78] ($d = 3$) and add support for control vectors to them.

Given a pure quadrilateral mesh, we generalise the univariate cubic stencils of Fig. 8 to the bivariate case. For vertices that are not extraordinary, we simply form tensor products of the univariate stencils. This gives rules for computing new vertex-, edge-, and face-points and vectors; see Fig. 12.

It remains to treat boundaries and extraordinary vertices (EVs), i.e., vertices where the valency is different from four and where the stencils of Fig. 12 do not apply. As our (semi-sharp) creases offer full approximation power and cubic reproduction (neither of which is offered by Pixar creases) in regular regions, it would be advantageous to maintain this property at boundaries as well. This can be achieved by using Bézier edge conditions obtained via multiple knots. This, however, puts constraints on positions of EVs: they cannot appear in the two-ring neighbourhoods of boundary curves. An alternative is to use sharp rules or ghost points. This allows EVs at boundaries, but reduces polynomial reproduction and approximation power.

Control vectors are not attached to extraordinary vertices, and so the regular vertex-point stencil (Fig. 12, top left) is replaced with the Catmull-Clark stencil for EVs. To allow control vectors at EVs, and thus to support creases running smoothly across extraordinary points, one would need to modify the natural configuration and characteristic map

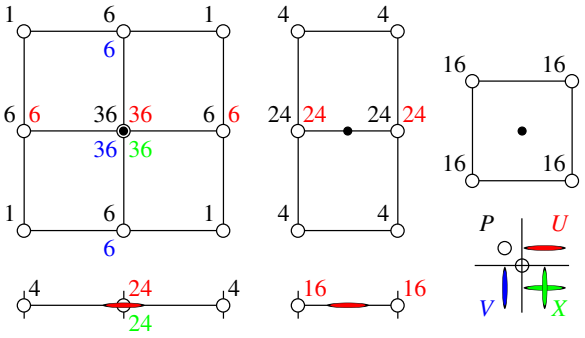

Figure 12: *Unnormalised bicubic stencils for control points and control vectors. Top row: Stencils for new vertex-, edge- and face-points. Bottom left: Stencil for new vertex control vector (the prolonged ellipses show the direction of the crease). Bottom centre: Stencil for new edge control vector. Bottom right: Our graphical notation for stencils. Contributions from P points (black) (i.e, the regular bicubic stencils) are shown in upper left relatively to old control points. Contributions from U (red) and V (blue) types of vectors are offset to upper right and lower left, respectively. Contributions of X (green) are offset to lower right. All weights should be normalised by* $1/64$*. Vertical control stencils (not shown) are the obvious analogues of the horizontal ones. The contribution of X to its refined version (not shown) is* $1/4$*.*

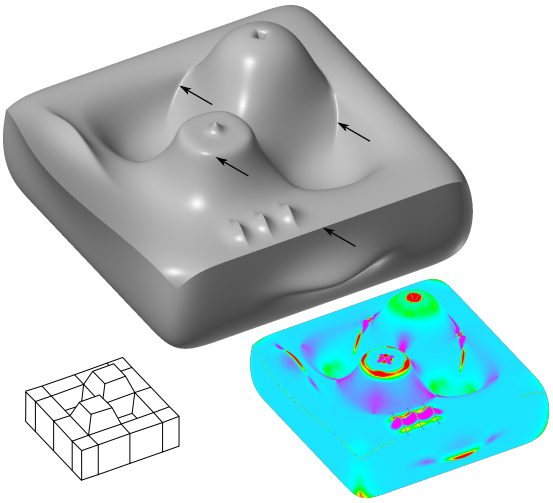

Figure 13: *A model with creases created using both semi-sharp Pixar rules (indicated by arrows) and our semi-sharp crease rules via control vectors (all other creases). A Gaussian curvature plot is also included, showing that our creases maintain the quality of the underlying surface.*

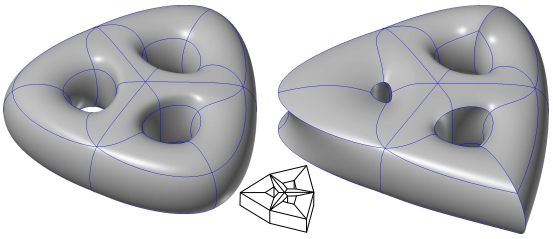

Figure 14: *A triple torus model (left; Catmull-Clark surface) with creases added via control vectors (right).*

[PR08] of the surface there. Our current solution is to allow for Pixar semi-sharp rules to be combined with our control vector rules. The affected stencils are then modified accordingly: new vertex and edge stencils are replaced by Pixar (semi-sharp) crease, dart, and corner rules [DKT98], as appropriate. An example of this synergy, including several multiresolution edits via control vectors and various sharpness values, is shown in Fig. 13 and in the supplementary video. Another example, created without Pixar rules, is shown in Fig. 14.

6. Discussion and future work

Traditional approximating splines hold the convex hull property as the corresponding basis functions partition unity and are non-negative. When control vectors are added (as e.g. in (11) and (15)), this property is lost. However, as the magnitudes of control vectors can be assumed to be bounded, it should be possible to design a more general enclosure (Section 13 of [Sab10]) using Minkowski sums or similar operations. Although convex hulls are important for interrogation, we do not see the lack of them as an issue for modelling or analysis.

As mentioned above, to be able to support creases through extraordinary points requires a modification of the natural configuration of the surface. Such investigation is beyond the scope of this paper.

In principle, it should be possible to generalise our method for creating (semi-sharp) creases to non-uniform subdivision. This would require an extension of the multi-stage algorithm designed in [CADS09, Cas10].

An interesting question is whether our method can be also applied to subdivision schemes based on box-splines, for example Loop subdivision [Loo87]. While box-splines do not natively support multiple knots, it should be possible to associate control vectors attached to control points with piecewise quartic splines with creases.

We reiterate that since crease functions (such as $\hat{N}_d$) are only added on top of the underlying blending functions (subdivision splines), polynomial reproduction and approximation power is not reduced in our method, compared to the creases developed in [Sta01, DKT98].

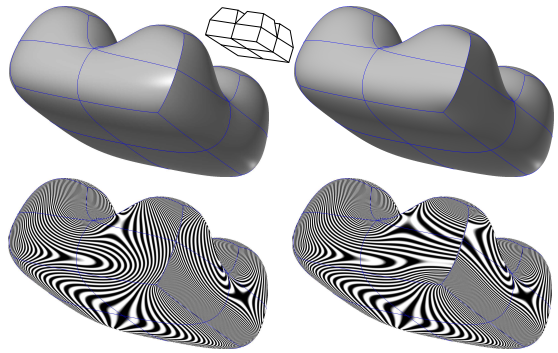

Figure 15: *A brick model with a crease. Left: Our result; Right: Result with Pixar crease rules. Note the flat portion of the crease created by Pixar crease rules. Our approach produces a fairer crease curve with better curvature behaviour of the surface (bottom).*

We compare Pixar and our creases in Fig. 15. As univariate Pixar crease rules create points with (one-sided) zero curvature [KSD14b], the surface has superior behaviour in the neighbourhood of our crease compared to Pixar creases.

7. Conclusion

We have devised methods for applying (semi-sharp) creases to curves and surfaces defined by subdivision schemes based on B-splines. Our approach generalises to arbitrary degree subdivision (including even degrees) and offers greater flexibility over existing methods via control vectors. As examples of our approach, we have demonstrated a new quintic scheme suitable for modelling curves with semi-sharp creases and demonstrated modifications to cubic surface subdivision that allow true multi-resolution editing and go beyond what Pixar and Stam's schemes offer.

Acknowledgement

This work was supported by the Engineering and Physical Sciences Research Council [EP/H030115/1].

References

[CADS09] CASHMAN T. J., AUGSDÖRFER U. H., DODGSON N. A., SABIN M. A.: NURBS with extraordinary points: high-degree, non-uniform, rational subdivision schemes. SIGGRAPH '09, ACM, pp. 46:1–46:9. 2, 9

[Cas10] CASHMAN T. J.: *NURBS-compatible subdivision surfaces*. Tech. Rep. UCAM-CL-TR-773, University of Cambridge, Computer Laboratory, Mar. 2010. (Doctoral thesis). 1, 2, 9

[CC78] CATMULL E., CLARK J.: Recursively generated B-spline surfaces on arbitrary topological meshes. *Computer-Aided Design 10*, 6 (1978), 350–355. 1, 8

[CLR80] COHEN E., LYCHE T., RIESENFELD R.: Discrete B-splines and subdivision techniques in computer-aided geometric design and computer graphics. *Computer Graphics and Image Processing 14*, 2 (1980), 87–111. 6

[COS00] CIRAK F., ORTIZ M., SCHRÖDER P.: Subdivision surfaces: a new paradigm for thin-shell finite-element analysis. *Int. J. Num. Methods in Engineering 47*, 12 (2000), 2039–2072. 1

[dB72] DE BOOR C.: On calculating with B-splines. *J. Approx. Theory 6*, 1 (1972), 50–62. 2

[DKT98] DEROSE T., KASS M., TRUONG T.: Subdivision surfaces in character animation. SIGGRAPH '98, ACM, pp. 85–94. 1, 2, 7, 9

[FB88] FORSEY D. R., BARTELS R. H.: Hierarchical B-spline refinement. SIGGRAPH '88, ACM, pp. 205–212. 5

[HDD*94] HOPPE H., DEROSE T., DUCHAMP T., HALSTEAD M., JIN H., MCDONALD J., SCHWEITZER J., STUETZLE W.: Piecewise smooth surface reconstruction. SIGGRAPH '94, ACM, pp. 295–302. 1

[HW11] HUANG Z., WANG G.: Non-uniform recursive Doo-Sabin surfaces. *Computer-Aided Design 43*, 11 (2011), 1527–1533. 2

[KSD14a] KOSINKA J., SABIN M. A., DODGSON N. A.: Control vectors for splines. *Computer-Aided Design* (2014). To appear. 1, 2, 5, 6, 7

[KSD14b] KOSINKA J., SABIN M. A., DODGSON N. A.: Creases and boundary conditions for subdivision curves. *Graphical Models* (2014). To appear, DOI: 10.1016/j.gmod.2014.03.004. 1, 2, 3, 4, 6, 7, 10

[KSD14c] KOSINKA J., SABIN M. A., DODGSON N. A.: Subdivision surfaces with creases and truncated multiple knot lines. *Computer Graphics Forum 23*, 1 (2014), 118–128. 1, 2

[LB07] LACEWELL D., BURLEY B.: Exact evaluation of Catmull-Clark subdivision surfaces near B-spline boundaries. *J. Graphics Tools 12*, 3 (2007), 7–15. 3

[Loo87] LOOP C.: *Smooth Subdivision Surfaces Based on Triangles*. M.S. thesis, University of Utah, 1987. 1, 9

[MFR*10] MÜLLER K., FÜNFZIG C., REUSCHE L., HANSFORD D., FARIN G., HAGEN H.: DINUS: Double insertion, nonuniform, stationary subdivision surfaces. *ACM Trans. Graph. 29* (July 2010), 25:1–25:21. 2

[MRF06] MÜLLER K., REUSCHE L., FELLNER D.: Extended subdivision surfaces: Building a bridge between NURBS and Catmull-Clark surfaces. *ACM Trans. Graph. 25* (April 2006), 268–292. 2

[PR08] PETERS J., REIF U.: *Subdivision Surfaces*. Springer Publishing Company, Incorporated, 2008. 9

[Sab10] SABIN M.: *Analysis and Design of Univariate Subdivision Schemes*. Springer, 2010. 5, 9

[Sta98] STAM J.: Exact evaluation of Catmull-Clark subdivision surfaces at arbitrary parameter values. SIGGRAPH '98, ACM, pp. 395–404. 1, 4

[Sta01] STAM J.: On subdivision schemes generalizing uniform B-spline surfaces of arbitrary degree. *Computer Aided Geometric Design 18*, 5 (2001), 383–396. 1, 2, 3, 4, 5, 7, 9

[SWZ04] SCHAEFER S., WARREN J., ZORIN D.: Lofting curve networks using subdivision surfaces. SGP '04, Eurographics, pp. 103–114. 2

[SZSS98] SEDERBERG T. W., ZHENG J., SEWELL D., SABIN M.: Non-uniform recursive subdivision surfaces. SIGGRAPH '98, ACM, pp. 387–394. 2